

Accepted Manuscript

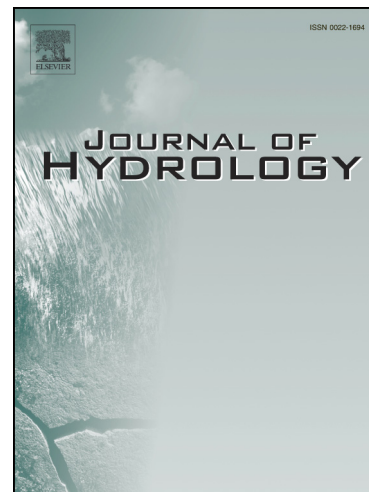
Evaluation of ensemble streamflow predictions in Europe

Lorenzo Alfieri, Florian Pappenberger, Fredrik Wetterhall, Thomas Haiden,
David Richardson, Peter Salamon

PII: S0022-1694(14)00495-8
DOI: <http://dx.doi.org/10.1016/j.jhydrol.2014.06.035>
Reference: HYDROL 19709

To appear in: *Journal of Hydrology*

Received Date: 2 December 2013
Revised Date: 7 May 2014
Accepted Date: 21 June 2014



Please cite this article as: Alfieri, L., Pappenberger, F., Wetterhall, F., Haiden, T., Richardson, D., Salamon, P., Evaluation of ensemble streamflow predictions in Europe, *Journal of Hydrology* (2014), doi: <http://dx.doi.org/10.1016/j.jhydrol.2014.06.035>

This is a PDF file of an unedited manuscript that has been accepted for publication. As a service to our customers we are providing this early version of the manuscript. The manuscript will undergo copyediting, typesetting, and review of the resulting proof before it is published in its final form. Please note that during the production process errors may be discovered which could affect the content, and all legal disclaimers that apply to the journal pertain.

Evaluation of ensemble streamflow predictions in Europe

Lorenzo Alfieri^{1,2}, Florian Pappenberger¹, Fredrik Wetterhall¹, Thomas Haiden¹, David Richardson¹, and Peter Salamon².

¹ European Centre for Medium-Range Weather Forecasts, Reading, UK

² European Commission - Joint Research Centre, Ispra, Italy

Correspondence to: Lorenzo Alfieri

European Commission - Joint Research Centre

TP 122, Via E. Fermi 2749

21027 Ispra (VA)

Italy

Tel: +39 0332 78 3835

Email: lorenzo.alfieri@jrc.ec.europa.eu

Abstract

In operational hydrological forecasting systems, improvements are directly related to the continuous monitoring of the forecast performance. An efficient evaluation framework must be able to spot issues and limitations and provide feedback to the system developers. In regional systems, the expertise of analysts on duty is a major component of the daily evaluation. On the other hand, large scale systems need to be complemented with semi-automated tools to evaluate the quality of forecasts equitably in every part of their domain.

This article presents the current status of the monitoring and evaluation framework of the European Flood Awareness System (EFAS). For each grid point of the European river

network, 10-day ensemble streamflow predictions are evaluated against a reference simulation which uses observed meteorological fields as input to a calibrated hydrological model.

Performance scores are displayed over different regions, forecast lead times, basin sizes, as well as in time, considering average scores for moving 12-month windows of forecasts.

Skilful predictions are found in medium to large rivers over the whole 10-day range. On average, performance drops significantly in river basins with upstream area smaller than 300 km², partly due to underestimation of the runoff in mountain areas. Model limitations and recommendations to improve the evaluation framework are discussed in the final section.

Keywords: flood early warning; ensemble streamflow predictions; CRPS; skill scores; distributed hydrological modelling.

ACCEPTED MANUSCRIPT

1 1 Introduction

2 Operational hydrological forecasting systems play a key role in the water resources
3 management and in the preparedness against extreme events. Assessing their performance is
4 crucial for the error diagnostic and in the planning of development work to improve the
5 system accuracy and extend the forecast lead time. A vast number of regional and national
6 hydro-meteorological centres have flood forecasting and early warning systems in place based
7 on weather predictions (see Alfieri et al., 2012 for a recent review of European systems). At
8 the same time, the number of ensemble-based systems is increasing (Cloke and Pappenberger,
9 2009; Wetterhall et al., 2013), with the aim of describing part of the uncertainty embedded in
10 the forecasts. The evaluation of the forecast accuracy is regularly performed in many
11 operational systems, where verification scores need to be complemented by the local
12 knowledge and experience of analysts on duty. Further, skill scores are rarely displayed
13 publicly, to prevent misinterpretation of results and avoid the need for simplifying their
14 information content for a wider recipient of users. Yet, reporting on past performance by
15 means of verification scores is listed as one of the main priorities of users, to increase the trust
16 in forecasting systems (Wetterhall et al., 2013).

17 Assessing the forecast performance over large domains raises the challenge of comparing
18 river points with different upstream area and hydrological regimes. In these cases, a
19 widespread approach to tackle the forecast verification is to compute scores based on the
20 probability of thresholds exceedance (e.g., warning levels), that can be defined in a consistent
21 way for every point. While this is a standard practice for early warning systems (e.g.,
22 Bartholmes et al., 2009; Gourley et al., 2012), it is also applied to the verification of
23 categorical events for any set of thresholds (Thirel et al., 2008). If quantitative values are
24 considered, the choice of performance scores becomes wider (Legates and McCabe, 1999;

25 Wilks, 2006), though only a relatively small subset is specifically dedicated to evaluate the
26 quality of ensemble forecasts (Brown et al., 2010). The comparison of forecast skill in several
27 river sections is often performed through benchmarking against simplified simulations
28 (Pappenberger et al., submitted), previous model versions (Arheimer et al., 2011), different
29 input data (e.g., Renner et al., 2009), or climatological values (Demargne et al., 2010;
30 Verkade et al., 2013; Wood et al., 2005). An alternative method consists in normalizing
31 forecasts and reference values before the evaluation (Pappenberger et al., 2010). Trinh et al.
32 (2013) used a similar concept to propose a modified Continuous Ranked Probability Score
33 (CRPS) which is suitable to compare forecast performance at different river sections. In
34 operational systems, the forecast performance must be monitored and updated continuously in
35 time. Hence, a skill assessment based on different scores and benchmarks (e.g., Alfieri et al.,
36 2013a; Randrianasolo et al., 2010) is often preferred in order to analyze different aspects of
37 the forecast performance at several locations and quickly detect trends over time or
38 weaknesses.

39 In 2012, after the transfer of the EFAS operational suite to the European Centre for Medium-
40 Range Weather Forecasts (ECMWF), a commitment was made to set up an evaluation
41 framework of the hydrological forecasts, in order to monitor their performance over time and
42 after major system updates. The idea was to implement an automated procedure to regularly
43 produce and update summary skill scores for the whole computation domain, able to spot a
44 variety of possible problems and address subsequent in-depth analysis. Among the main
45 challenges to face was the choice of appropriate skill scores, the handling of large data sets,
46 and the visualization of results through concise and intuitive graphs.

47 This article presents the current status of implementation of such an evaluation framework,
48 after one year of operational runs at ECMWF. Streamflow forecasts at every grid point of the

49 river network are verified against a reference simulation which uses observed meteorological
50 fields as input to a calibrated hydrological model.

51 **2 Data and Methods**

52 **2.1 Model framework**

53 The main components of the EFAS hydro-meteorological forecasting chain are: a) a
54 hydrological model, b) weather forecasts, and c) meteorological observations, to update the
55 initial model states and for verification purpose (see Figure 1). Each of these three
56 components has inherent uncertainty, which can be described in the modelling framework and
57 propagated to the output discharge. The current EFAS system is a multi-model ensemble
58 approach, in that it accounts for the uncertainty of input weather forecasts using model runs
59 from different meteorological centres in Europe. These include two deterministic forecasts,
60 from the ECMWF (ECMWF-HiRes, Miller et al., 2010) and from the German Weather
61 Service (DWD, see Majewski et al., 2002; Steppeler et al., 2003), and two ensemble forecasts,
62 from the COSMO Consortium (COSMO-LEPS, Marsigli et al., 2005) and from ECMWF
63 (ECMWF-ENS, Miller et al., 2010). The version of the evaluation framework presented here
64 is based on the performance of the ECMWF-ENS forecasts only, though it is foreseen to
65 extend it to include the other model simulations. The system setup and additional details on
66 how weather forecasts are handled in EFAS are documented in the published literature
67 (Bartholmes et al., 2009; Pappenberger et al., 2010; Thielen et al., 2009), therefore we refer
68 the reader to these articles for additional information not included in the present work, and
69 focus on the analysis of the evaluation framework.

70

71 *Figure 1: Schematic view of the EFAS hydro-meteorological forecasting system.*

72 2.2 Meteorological data

73 ECMWF-ENS is a 51-member ensemble forecast run twice per day, at 00 UTC and 12 UTC
74 as part of the operational production suite of ECMWF Integrated Forecast System (IFS, see
75 Bechtold et al., 2014; Miller et al., 2010). ENS forecasts are run globally at T639 spectral
76 resolution, corresponding to about 32 km horizontal resolution, with forecast lead time (LT)
77 up to 10 days. After day 10, the model run is extended up to day 15 (day 32 twice per week)
78 at a coarser horizontal resolution of about 65 km. Currently, EFAS uses only the first 10 days
79 of forecast as input to the hydrological model. For this work, ENS forecasts from January
80 2009 to the present were extracted and used in the hydrological simulations, considering those
81 available at the time of the forecasts (i.e., no reforecast with more recent IFS versions was
82 used). Meteorological forecast fields used are total precipitation, evaporation, and 2-metre
83 temperature, which are regridded to the same spatial resolution of the hydrological model (see
84 next section).

85 A database of observed meteorological fields for Europe was provided by the Joint Research
86 Centre of the European Commission. It consists of maps of spatially interpolated point
87 measurements of precipitation and temperature at the surface level. The database includes
88 daily data from the 1990 to the present, and it is populated by an increasing number of
89 reporting gauges over time, with the latest figures showing on average more than 6000
90 stations for precipitation and more than 4000 for temperature (see Figure 2 for a recent
91 example of daily data). A subset of the same meteorological station network is used to
92 generate interpolated potential evapotranspiration maps using the Penman-Monteith method.

93
94 *Figure 2: stations reporting observed precipitation (left) and average temperature (right) on*
95 *the 1st October 2013.*

96

97 **2.3 Hydrological modelling**

98 In EFAS, hydrological simulations are performed with Lisflood, a hybrid between a
99 conceptual and a physical rainfall–runoff distributed model, designed to reproduce the main
100 hydrological processes of medium to large river basins (see van der Knijff et al., 2010). The
101 considered model setup for Europe was calibrated at 481 river gauges, using the observed
102 meteorological fields as input and up to 7 years of gauged discharge. A reference hydrological
103 simulation starting in 1990 was run for the European window with the calibrated Lisflood
104 model at 5x5 km resolution, using the observed meteorological fields as input. The
105 operational model is updated daily using the initial states of the previous day and the most
106 recent meteorological observations acquired with about 1 day lag. This simulation, hereafter
107 referred to as EFAS Water Balance (EFAS-WB), represents our best estimate of the
108 hydrological states in the European rivers. The EFAS-WB is used in EFAS with regard to
109 three main aspects (see Figure 1): *I*) deriving climatological features of the runoff in each
110 point of the river network (e.g., average conditions, extremes, alert thresholds, seasonality);
111 *II*) creating initial conditions for daily hydrological runs driven by the latest weather
112 predictions; *III*) providing a reference simulation which is as realistic as possible, to be used
113 as a proxy to evaluate streamflow forecasts in every grid point of the simulation domain.
114 Further details on the EFAS-WB are described by Alfieri et al. (2013b). The same calibrated
115 Lisflood setup is used to perform 10-day EFAS streamflow forecasts updated twice per day,
116 by forcing the hydrological model with initial conditions from the EFAS-WB and with
117 forecast weather fields (described in the previous section) with 1-day temporal resolution.

118 3 Evaluation strategy

119 EFAS forecasts are run at the ECMWF twice per day since October 2012, using weather
120 predictions initialized at 00 and 12 UTC. This operational dataset of hydrological forecasts
121 was complemented by running 4 years of daily hindcasts with the same model configuration,
122 starting on January 2009. To reduce the computing load, the hindcasts were run only once per
123 day, using forecast runs from 12 UTC. Ensemble streamflow predictions (ESP) are validated
124 against the EFAS-WB for each point of the modelled European river network, comprising
125 38452 grid points. Such an approach enables a quick spatial overview of skill scores on every
126 region of the computation domain, rather than just at stations where observed discharge is
127 provided. On the other hand it does not account for the potential mismatch between actual
128 river discharge and the simulated EFAS-WB used as reference.

129 Average scores are calculated over 1-year time windows. This choice proved to be effective
130 as it includes one full hydrological year and dampens the seasonal variability of skill scores.
131 In practice, the verification of dry months leads to higher scores than those of rainy months,
132 as the quantitative forecast of high precipitation amounts is more challenging than forecasting
133 days with zero precipitation. As a result, the evaluation framework was set up to select the
134 first day of each month and calculate the average skill scores of the previous 365 days,
135 starting on the 1st January 2010. The procedure was then semi-automated and skill scores are
136 now updated every month to include results of the latest forecasts.

137 Skill scores to evaluate the ESP were chosen so that grid points with different upstream area
138 and climatic regime could be compared together in the same graphs and in the same maps. To
139 this end, four different dimensionless skill scores were selected, able to stress different
140 aspects of the forecast performance. These are described in the following sub-sections and
141 summarized in Table 1.

142 3.1 Nash-Sutcliffe efficiency

143 The Nash-Sutcliffe efficiency (NS, Nash and Sutcliffe, 1970) applied to discharge forecasting
 144 can be defined as:

$$145 \quad NS = 1 - \frac{\sum_{t=1}^N [q_{sim}(t) - q_{fc}(t)]^2}{\sum_{t=1}^N [q_{sim}(t) - \bar{q}_{sim}]^2}, \quad (1)$$

146 where q_{sim} is the proxy discharge given by the EFAS-WB and q_{fc} is the forecast discharge at
 147 the same time step. t is a time index spanning all N forecasts included in the evaluation
 148 window, that is $N=730$ in operational forecasts (when two forecasts per day are evaluated)
 149 and $N=365$ for hindcasts between 2009 and 2012. In the case of the considered ESP, q_{fc}
 150 represents the mean of the 51-member ensemble. The NS values range from $-\infty$ to 1, the latter
 151 corresponding to perfect forecasts. NS above 0 means that forecasts perform better than
 152 climatological values, in the form of their average discharge \bar{q}_{sim} . In the presented work, NS
 153 values are calculated for fixed forecast lead times between 1 and 10 days, and the average
 154 values over 1 year windows are shown, as described in the previous section.

155 3.2 Forecast bias

156 Monitoring the bias of ensemble streamflow predictions is of vital importance for a flood
 157 awareness system based on a threshold exceedance approach as in EFAS. Flood alerts are
 158 detected by comparing EFAS simulations driven by weather forecasts as input, against
 159 reference warning thresholds, derived from the EFAS-WB. If weather forecasts were
 160 persistently different from observed meteorological values, discharge forecasts would be
 161 consequently biased, which may result in statistically significant over- or under-prediction of
 162 flood alerts. The main potential source of bias in ESP is the quantitative forecast of
 163 precipitation, particularly for high flow events. However, biased forecast values of
 164 temperature may induce cyclical drifts of discharge predictions, particularly in hydrological

165 regimes where the snow accumulation and melting processes play a prominent role. In
 166 addition, precipitation, temperature and evapo-transpiration are key drivers for the soil
 167 moisture state, therefore consistent bias in their forecast values can affect the streamflow
 168 potentially over long ranges (i.e., monthly to inter-annual time scales). In the presented
 169 evaluation framework, the bias at each grid point is rescaled by the corresponding average
 170 discharge for the same period, calculated from the EFAS-WB:

$$171 \quad \mathbf{Pbias} = \frac{\frac{1}{N} \sum_{t=1}^N [q_{sim}(t) - q_{fc}(t)]}{\bar{q}_{sim}} \quad (2)$$

172 Being a linear operator, the sum of the percentage bias (Pbias) of all ensemble members is
 173 equal to the percentage bias of the ensemble mean.

174 3.3 Coefficient of variation of the RMSE

175 The Root Mean Squared Error (RMSE) has long been used to assess the magnitude of the
 176 error of deterministic forecasts. It has the advantage that it retains the units of the forecast
 177 variable and it includes the effect of both bias and variance of estimation. In addition, the
 178 RMSE depends on a quadratic function of the estimation residuals. This lead to some
 179 peculiarities, among which: 1) it is highly affected by few large errors and 2) it is often used
 180 as an error function to be minimized in a wide range of calibration and optimization
 181 processes. On the other hand it is difficult to compare RMSE values among different river
 182 stations, as their climatological discharge values may be substantially different. One option to
 183 compare the RMSE at different locations is to rescale it by the corresponding average
 184 discharge, as shown in Reed et al. (2007), so that resulting values become dimensionless:

$$185 \quad \mathbf{CV} = \frac{\sqrt{\frac{\sum_{t=1}^N [q_{sim}(t) - q_{fc}(t)]^2}{N}}}{\bar{q}_{sim}}, \quad (3)$$

186 The resulting score is commonly referred to as coefficient of variation (CV) of the RMSE
 187 and, as for the RMSE, values close to zero are preferable. Also, when CV values are close to
 188 1 it means that the RMSE of estimation is of the same order as the average discharge. Indeed,
 189 it can be associated to an inverse of the signal-to-noise ratio. By definition the CV penalizes
 190 river reaches with low average discharge compared to its variability, therefore higher CV
 191 values are expected in small or flash-flood prone river basins, such as those along the
 192 Mediterranean coast, where the predictability is indeed shorter than in large river basins.

193 3.4 Continuous Ranked Probability Skill Score

194 To fully exploit and assess the added value of probabilistic predictions, the Continuous
 195 Ranked Probability Skill Score (CRPSS) is used to evaluate the quantitative skills of the ESP.

196 The CRPSS (e.g., Hersbach, 2000) is defined as:

$$197 \quad CRPSS = \frac{\overline{CRPS_{ref}} - \overline{CRPS_{forecast}}}{\overline{CRPS_{ref}}}, \quad (4)$$

198 where

$$199 \quad CRPS = \int_{-\infty}^{\infty} [F(y) - F_0(y)]^2 dy \quad (5)$$

200 and

$$201 \quad F_0(y) = \begin{cases} 0, & y < \text{observed value} \\ 1, & y \geq \text{observed value} \end{cases} \quad (6)$$

202 while $F(y)$ is the stepwise cumulative distribution function (cdf) of the ESP of each
 203 considered forecast. The CRPSS is a dimensionless indicator of the skill of ensemble
 204 predictions, measured by $(\overline{CRPS_{forecast}})$, compared to that of a reference forecast $(\overline{CRPS_{ref}})$.

205 The CRPSS ranges between 1 (for perfect predictions) to $-\infty$, though ESP are valuable only
 206 when $CRPSS > 0$, i.e., when the forecasts perform better than the reference. In this work, we
 207 compare and discuss the use of two different $\overline{CRPS_{ref}}$ to evaluate the CRPSS, the first based

208 on the average climatological discharge \bar{q}_{sim} ($CRPS_{ref,ad}$), and the second based on a
 209 persistence forecast ($CRPS_{ref,pf}$), meaning a forecast given by assuming the same value used to
 210 initialize the ESP. It is worth noting that both reference CRPS are based on deterministic
 211 predictions, hence the $CRPS_{ref}$ reduces to the mean absolute error (Hersbach, 2000):

$$212 \quad CRPS_{ref,ad} = \frac{1}{M} \sum_{t=1}^M |q_{sim}(t) - \bar{q}_{sim}| \quad (7)$$

213 where t is a daily time index going from 1/1/1990 to the present. On the other hand,

$$214 \quad CRPS_{ref,pf}(LT) = \frac{1}{N} \sum_{t=1}^N |q_{sim}(t) - q_{sim}(t - LT)| \quad (8)$$

215 where N has the same meaning as in Eq.1.

216 Two significant differences between Eq.7 and 8 can be seen. The $CRPS_{ref,ad}$ is a constant
 217 value and only depends on the location, though it needs climatological information to be
 218 evaluated, in the form of a reference time series of observations or proxy simulations (i.e., the
 219 EFAS-WB in this case). On the other hand, the $CRPS_{ref,pf}$ depends on the lead time of the
 220 forecast (LT). It does not need any prior climatological information on the discharge regime
 221 at the point but the discharge value used to initialize the forecast.

222 4 Results

223 Skill scores of the last available year are now routinely calculated on the 13th day of each
 224 month, after all meteorological observations to update the EFAS-WB are received and the
 225 hydrological model is run. Simulated proxy discharges need to be computed until the 11th of
 226 the same month, so that 10-day ESP starting on the 1st can be evaluated. Scores described in
 227 Sect. 3 are shown in **Figure 3**. NS, CV and Pbias are deterministic scores; hence they are
 228 calculated on the ensemble mean, while the CRPSS take into account the whole ensemble. A
 229 forecast lead time of 5 days is chosen for most figures in the article, being representative of
 230 the general behaviour of the ESP and a frequent lead time of EFAS flood alerts. One can see

231 that, for $LT=5$ days, in the vast majority of grid points the ESP is more skilful than a
232 persistence forecast (i.e., $CRPSS_{pf}>0$). The NS and the CV suggest that higher performance is
233 achieved in large rivers of Central and Northern Europe. Excluding Iceland, lower skills are
234 mostly seen in Southern Europe and can be explained by a) resolution issues in small basins,
235 b) less skilful precipitation forecast in mountainous areas, c) a comparatively lower station
236 density to run the EFAS-WB, and d) the higher proportion of convective precipitation,
237 leading to higher space-time variability of rainfall rates and larger extremes over short (i.e., 1-
238 day or sub-daily) durations. Similarly, the Pbias (on gray background in **Figure 3**) shows a
239 widespread underestimation of discharge over the main mountain ranges (i.e., Pyrenees, Alps
240 and Balkans, among others), mostly in the range 10% to 50% of the corresponding average
241 flow. These findings are in line with previous works by Wittmann et al. (2010) and
242 Pappenberger et al. (2013), who showed increasing underestimation of precipitation and
243 streamflow forecast in the Alpine region during intense precipitation events. The apparently
244 poor performance over Iceland in **Figure 3** is actually imputable to an incorrect reference
245 streamflow. Indeed, the number of reporting stations for this region is very low (see an
246 example in **Figure 2**), particularly for precipitation, thus leading to a considerable under-
247 prediction of the streamflow. In other words, although EFAS streamflow forecasts over
248 Iceland may be skilful, the current availability of meteorological observations prevents from
249 simulating reliable reference discharge to perform forecast evaluation in this area. In the
250 following analyses, summary scores of grid points in Iceland are excluded from all figures,
251 which brings the dataset to a subset of 37588 points.

252

253 *Figure 3: $CRPSS_{pf}$, CV, NS and Pbias over Europe for 1 year of daily forecasts ending on the*
254 *1st October 2013 (5-day lead time).*

255 4.1 Performance versus forecast range

256 Skill scores as in **Figure 3** are shown in **Figure 4** for each forecast lead time between 1 and
257 10 days. A solid line indicates the mean value among all grid points, while grey shades denote
258 the 5%-95% (light grey) and the 25%-75% (dark grey) of their distribution. In the top-left
259 panel, the CRPSS calculated using the average discharge as reference (i.e., $CRPSS_{ad}$) is
260 shown with a thick dashed line (mean value) together with the corresponding 25%-75%
261 values (dotted lines). Differences between the two methods are the largest for the first lead
262 time, where in many cases the ESP does not bring substantial differences in comparison to a
263 persistence forecast, due to the large weight of the initial model states. On the other hand, the
264 $CRPSS_{ad}$ decreases roughly linearly and suggests the presence of a crossing point for a $LT > 10$
265 days, when the climatological average discharge seems to become a more skillful benchmark
266 than a persistence forecast. As expected, the CV tends to deteriorate with the lead time,
267 though without a significant increase of the spread of its distribution. Similarly, the mean NS
268 ranges between 0.9 for $LT=1$ and 0.7 at the end of the forecast range, while in 99% of
269 forecasts $NS > 0$ for $LT=10$ days. The Pbias shows a rather constant mean under-prediction of
270 2% to 4%. Its distribution has an increasing spread with the lead time, with 65% to 70% of
271 grid points lying constantly below the zero line.

272

273 *Figure 4: CRPSS, CV, NS and Pbias of ESP versus the forecast lead time.*

274

275 4.2 Performance versus catchment size

276 **Figure 5** displays the four scores against the upstream area of each grid point, calculated over
277 1 year ending on 1/10/2013 and for a 5-day lead time. In addition, solid lines indicate the
278 empirical median value (i.e., 50th percentile), in light grey, and the central 90% of the

279 distribution (i.e., 5th to 95th percentiles), in dark grey. Largest values on the x-axis
280 correspond to the lower Danube River, with upstream area up to about 800,000 km². On the
281 left side of each panel, one can note the model grid resolution as limit, with catchments area
282 being always a multiple of 25 km². Results in **Figure 5** denote a general positive trend of skill
283 scores with increasing upstream area. Indeed, in large rivers, a) the discharge varies more
284 gradually due to the smoothing and averaging effect of the complex river network and b) the
285 influence of the initial discharge, compared to the forecast precipitation input, is larger than in
286 smaller catchments. In detail, as the basin time of concentration increases and approaches the
287 magnitude of the forecast range, a larger proportion of the forecast discharge at the river
288 outlet is made up by a water volume which is already in the model, (i.e., gauged) at the
289 starting time of the forecast run. Therefore the skill of weather forecasts affects that of
290 streamflow forecasts with an average delay increasing with the upstream area, which can be in
291 the order of some days for large European rivers. On the other hand, **Figure 5** shows a clear
292 deterioration of scores for catchments smaller than 300 km², that is, for a ratio between
293 upstream area and grid size of the weather forecasts of about 0.3. Results are in agreement
294 with those of Pappenberger et al. (2010), though Bartholmes et al. (2006) suggested a
295 minimum threshold of 4000 km² if extreme values are considered. Indeed, the latter value is
296 used in EFAS as minimum upstream area for flood alerts to be issued to partner institutes.
297 The median value of the Pbias in **Figure 5** indicates that the deterioration of scores can be
298 partly attributed to the underestimation of the discharge for small catchments, which
299 decreases below 2%, in absolute value, for upstream areas larger than 400 km². As
300 commented in Sect. 4, such trend is to be attributed to the under-prediction of quantitative
301 precipitation in mountain areas and of extreme values in general, not fully captured by the
302 atmospheric circulation model due to its grid size on average coarser than the observation
303 network.

304

305 *Figure 5: CRPSS_{pf}, CV, NS and Pbias of ESP versus the upstream area of each river grid*306 *point.*

307

308 **4.3 Evolution of 12-month average performance**

309 The evolution of summary scores over the past 5 years is shown in **Figure 6**. Scores are
310 calculated on the 365 days preceding the first day of each month indicated in the x axis. In the
311 top-left panel both $CRPSS_{pf}$ and $CRPSS_{ad}$ are shown, using the same line types as in **Figure 4**.
312 In addition, the average discharge over all grid points of the river network, for each evaluation
313 period, is drawn at the bottom. One can note how the $CRPSS_{ad}$ is largely affected by the
314 magnitude of the observed runoff, so that, in drier years, it gives the impression of increasing
315 forecast performance, and vice-versa. In the $CRPSS_{pf}$, no dependence on the average runoff is
316 visible. The latter shows an improvement of the forecast skills during the year 2013,
317 particularly for the mean of the distribution and for the 75th and 95th quantiles. Such
318 improvement is also pointed out by a reduced mean CV and increased mean NS, where in
319 both cases the central 90% of the distribution becomes narrower since the beginning of 2013,
320 though with a subsequent widening towards the end of the year.

321 Interestingly, the bottom-right panel denotes a slow but constant increase of a negative bias in
322 forecast streamflow over the last years. This appears consistently on all lead times (not
323 shown), though it is more significant towards the end of the forecast range. On the other hand,
324 no corresponding trend was reported in the forecast input precipitation produced by the
325 ECMWF-ENS (personal communication, see some additional details in
326 <http://www.ecmwf.int/products/forecasts/d/charts/medium/verification>), nor in temperature
327 (possibly inducing a larger snow fraction). Instead, the main reason for such discrepancy is

328 most likely due to the progressive increase in the number of stations reporting meteorological
329 observations in recent years. Higher station density leads to a more realistic representation of
330 the input maps to run the EFAS-WB, so that small-scale features such as convective cells are
331 more likely to be better observed quantitatively. In this regard, Kann and Haiden (2005)
332 showed that when high density stations networks are used as reference, the mean absolute
333 error of forecast precipitation tend to increase with the reduction of the aggregation area.
334 Further, some of the stations added recently are located in elevated areas, such as in the Alps
335 and the Pyrenees, where the orography enhances annual rainfall totals and consequently the
336 runoff. Indeed, these areas are where the under-prediction of discharges has become clearer in
337 the recent years, as shown in **Figure 3**.

338

339 *Figure 6: Trend of 12-month average CRPSS, CV, NS and Pbias of ESP from 2009 onwards.*

340

341 **5 Discussion and conclusions**

342 This article presents the current status of the evaluation framework used to monitor and
343 update regularly the forecast performance of the European Flood Awareness System. Results
344 suggest that streamflow forecasts driven by weather predictions provide significant added
345 value to the monitoring of the main European rivers. As expected, performance decreases
346 with lead time, though it remains skilful for the whole 10-day range, in comparison to the use
347 of climatological or persistence forecasts. In large river basins of Europe, the average time lag
348 between weather forcing and runoff is on the order of some days. Hence the real-time
349 hydrological simulation run with meteorological observations gives a significant proportion of
350 the overall predictability, increasing with the basin time of concentration. In smaller river
351 basins, the effect of initial conditions is less important, therefore the predictability is shorter

352 as it mostly depends on that of the weather forecasts. In river basins of size below 300-400
353 km² forecast skill becomes poorer. Their forecasts show large variability, often even for 1-day
354 lead time, and significant underestimation of the runoff in mountain regions.

355 Being designed on dimensionless scores, the main strength of the proposed verification
356 system is in highlighting relative changes of performance, which can be detected over
357 different regions, forecast lead time, basin size and, most importantly, in time. An evaluation
358 of 12-month average scores over the past 5 years suggests a moderate improvement for all 12-
359 month forecasts ending from the beginning of 2013 onwards. Such improvement occurred
360 notwithstanding an increasing negative forecast bias, especially in mountain regions. This can
361 be attributed to a progressive increase of the meteorological stations used to run the EFAS-
362 WB, which in turn has improved the representation of the runoff dynamics in the presence of
363 pronounced orography. Although the parameterization of the hydrological model was subject
364 to changes and improvements every 1 to 1.5 years on average, the 5 year simulation shown in
365 this study was carried out with a fixed model version, corresponding to the current operational
366 one at the time of writing. Therefore, the positive trend of performance shown in **Figure 6** is
367 likely to underestimate the real improvements which have occurred and rather reflect that of
368 weather forecasts used as input.

369 **5.1 The benchmark of skill scores**

370 The four performance scores presented in the article can be classified into two categories,
371 depending on whether the comparison is carried out against a benchmark or not. On the one
372 hand, the CV and the Pbias give a measure of the RMSE and of the bias of forecasts,
373 respectively. RMSE and bias are commonly used in verification because of their physical
374 meaning, as they quantify the error with the same units of the forecast variable. They are
375 rescaled by the average flow to make them comparable over different regions and along the

376 river network. On the other hand, the NS and the CRPSS give a relative performance in
 377 comparison to an alternative benchmark forecast. Literature works show a surprising variety
 378 of different benchmarks used for comparison (see Pappenberger et al., submitted, for a recent
 379 review), sometimes without motivating the choice. Here we argue that, in assessing the
 380 predictability of a forecasting system, the benchmark should represent a realistic forecast
 381 achievable in case the system was not in place. The use of persistence forecasts is hereby
 382 suggested as a suitable benchmark, in that it does not require climatological information of
 383 the runoff at the river point, nor additional model runs. In comparison to a benchmark based
 384 on the average discharge, persistence acknowledges the role of initial conditions, indicating
 385 that the highest value of forecasts corresponds to a balance between the ability to provide
 386 accurate forecasts and the ability to detect deviations from an initial state (see $CRPSS_{ad}$ versus
 387 $CRPSS_{pf}$ in **Figure 4**). Further, persistence is independent of seasonal variations or trends in
 388 the mean value of the forecast variable, as discussed in Sect. 4.3.

389 It is worth noting that the same principle can be applied to the Nash-Sutcliffe efficiency, as
 390 suggested by Plate and Lindenmaier (2008), leading to a modified formulation which uses a
 391 persistence forecast as reference value:

$$392 \quad NS(LT) = 1 - \frac{\sum_{t=1}^N [q_{sim}(t) - q_{fc}(t)]^2}{\sum_{t=1}^N [q_{sim}(t) - q_{sim}(t-LT)]^2} \quad (9)$$

393 This formulation was not tested in the present framework, though it may be a valid alternative
 394 to the NS for large river basins (see e.g., Pagano, 2013). Its application will be considered for
 395 future system developments.

396 **5.2 The EFAS-WB as reference simulations**

397 The main assumption of the presented approach is that the EFAS-WB can be used as a
 398 realistic representation of the actual runoff. On the other hand the use of the output of a

399 distributed model as the EFAS-WB allows a performance evaluation over the full
400 computation domain. Moreover, the continuous increase in the number of reporting stations,
401 both for meteorological and hydrological data, is progressively pushing the EFAS-WB closer
402 to the real streamflow conditions in the European rivers. This occurs thanks to a better
403 reproduction of the meteorological input data and to the increase of the number of river
404 stations where the parameters of the hydrological model can be calibrated. Recent advances in
405 the meteorological dataset include the addition of more than 10 high density national
406 networks and an improved approach to interpolating point values into spatial maps (see
407 Ntegeka et al., 2013). This is currently being tested and will be used in the next version of
408 EFAS, together with additional historical observed streamflow at a number of river gauges to
409 improve the model calibration. Similarly, resulting simulated discharges of the EFAS-WB can
410 potentially become a dataset to validate and benchmark a wide range of hydrological models,
411 particularly on large scales. Current main limitations of simulated discharges are at the lower
412 end of the range of the space-time scale of simulated catchments. In fact, the current daily
413 time aggregation of input data induces a smoothing of output discharges, so that simulated
414 extreme values have reported under-estimation issues, relatively to observed values. In
415 addition, the presented scores are not able to capture potential errors in the hydrological
416 model, because both ESP and the EFAS-WB used for validation are generated by the same
417 model. However, this is evaluated separately at those stations where the model parameters are
418 calibrated (see Feyen et al., 2007). Also, an assessment of the total predictive uncertainty is
419 performed at river gauges (currently about 40) where discharge values are received in real-
420 time. The methodology and results are described by Bogner and Pappenberger (2011).

421 5.3 Concluding remarks

422 In its current state, the evaluation framework has proved its usefulness in spotting strengths
423 and weaknesses of ensemble forecasts used in EFAS, including trends of performance in time
424 and size limits of river basins under monitoring. In addition, it has pointed out a number of
425 key developments to focus on to improve the evaluation and the diagnostic of the forecasting
426 system:

427 - Implementation of the evaluation framework to streamflow predictions derived from all the
428 different numerical weather predictions used as input in EFAS, including DWD, COSMO-
429 LEPS and products which are foreseen to be tested in the future.

430 - Enlarging the collection of near real time observed discharges for continuous monitoring of
431 the skill scores of both the EFAS-WB and streamflow predictions against observed values.

432 - Comparison of performance scores for updated model versions. A new EFAS version was
433 implemented in January 2014, which includes a more extensive calibration of the
434 hydrological model and an enhanced dataset of meteorological observations.

435 - Complementing the current approach with skill scores targeted to evaluate the performance
436 in forecasting extreme events, including threshold exceedance analyses.

437 - Set up a visualization platform on the web where performance can be monitored by
438 developers, analysts on duty and users, to aid the monitoring of forecasts and the diagnostic of
439 issues.

440

441 **References**

- 442 Alfieri, L., Burek, P., Dutra, E., Krzeminski, B., Muraro, D., Thielen, J. and Pappenberger, F.,
443 2013a. GloFAS – global ensemble streamflow forecasting and flood early warning, *Hydrol.*
444 *Earth Syst. Sci.*, 17, 1161–1175, doi:10.5194/hess-17-1161-2013,.
- 445 Alfieri, L., Salamon, P., Bianchi, A., Neal, J., Bates, P. and Feyen, L., 2013b. Advances in
446 pan-European flood hazard mapping, *Hydrol. Process.*, doi:10.1002/hyp.9947.
- 447 Alfieri, L., Salamon, P., Pappenberger, F., Wetterhall, F. and Thielen, J., 2012. Operational
448 early warning systems for water-related hazards in Europe, *Environ. Sci. Policy*, 21, 35–49.
- 449 Arheimer, B., Lindström, G. and Olsson, J., 2011. A systematic review of sensitivities in the
450 Swedish flood-forecasting system, *Atmos. Res.*, 100, 275–284.
- 451 Bartholmes, J. C., Thielen, J., Ramos, M. H. and Gentilini, S., 2009. The European flood alert
452 system EFAS - Part 2: Statistical skill assessment of probabilistic and deterministic
453 operational forecasts, *Hydrol. Earth Syst. Sc.*, 13, 141–153.
- 454 Bartholmes, J., Thielen, J. and Ramos, M. H., 2006. Quantitative analyses of EFAS forecasts
455 using different verification (skill) scores, The benefit of probabilistic flood forecasting on
456 European scale, edited by: Thielen, J., EUR, 22560, 58–79.
- 457 Bechtold, P., Semane, N., Lopez, P., Chaboureau, J.-P., Beljaars, A. and Bormann, N., 2014.
458 Representing equilibrium and nonequilibrium convection in large-scale models, *J. Atmos.*
459 *Sci.*, 71, 734–753, doi:10.1175/JAS-D-13-0163.1.
- 460 Bogner, K. and Pappenberger, F., 2011. Multiscale error analysis, correction, and predictive
461 uncertainty estimation in a flood forecasting system, *Water Resour. Res.*, 47, W07524,
462 doi:10.1029/2010WR009137.

- 463 Brown, J. D., Demargne, J., Seo, D.-J. and Liu, Y., 2010. The Ensemble Verification System
464 (EVS): A software tool for verifying ensemble forecasts of hydrometeorological and
465 hydrologic variables at discrete locations, *Environ. Modell. Softw.*, 25, 854–872,
466 doi:10.1016/j.envsoft.2010.01.009.
- 467 Cloke, H. L. and Pappenberger, F., 2009. Ensemble flood forecasting: A review, *J. Hydrol.*,
468 375, 613–626.
- 469 Demargne, J., Brown, J., Liu, Y., Seo, D.-J., Wu, L., Toth, Z. and Zhu, Y., 2010. Diagnostic
470 verification of hydrometeorological and hydrologic ensembles, *Atmos. Sci. Lett.*, 11, 114–
471 122.
- 472 Feyen, L., Vrugt, J. A., Nualláin, B., van der Knijff, J. and De Roo, A., 2007. Parameter
473 optimisation and uncertainty assessment for large-scale streamflow simulation with the
474 LISFLOOD model, *J. Hydrol.*, 332, 276–289, doi:10.1016/j.jhydrol.2006.07.004.
- 475 Gourley, J. J., Erlingis, J. M., Hong, Y. and Wells, E. B., 2012. Evaluation of Tools Used for
476 Monitoring and Forecasting Flash Floods in the United States, *Weather Forecast.*, 27, 158–
477 173, doi:10.1175/WAF-D-10-05043.1.
- 478 Hersbach, H., 2000. Decomposition of the continuous ranked probability score for ensemble
479 prediction systems, *Weather Forecast.*, 15, 559–570.
- 480 Kann, A. and Haiden, T., 2005. The August 2002 flood in Austria: sensitivity of precipitation
481 forecast skill to areal and temporal averaging, *Meteorol. Z.*, 14, 369–377, doi:10.1127/0941-
482 2948/2005/0042.
- 483 Van der Knijff, J. M., Younis, J. and de Roo, A. P. J., 2010. LISFLOOD: A GIS-based
484 distributed model for river basin scale water balance and flood simulation, *Int. J. Geogr. Inf.*
485 *Sci.*, 24, 189–212.

- 486 Legates, D. R. and McCabe, G. J., 1999. Evaluating the use of “goodness-of-fit” Measures in
487 hydrologic and hydroclimatic model validation, *Water Resour. Res.*, 35, 233–241,
488 doi:10.1029/1998WR900018.
- 489 Majewski, D., Liermann, D., Prohl, P., Ritter, B., Buchhold, M., Hanisch, T., Paul, G.,
490 Wergen, W. and Baumgardner, J., 2002. The operational global icosahedral-hexagonal
491 gridpoint model GME: Description and high-resolution tests, *Mon. Weather Rev.*, 130, 319–
492 338.
- 493 Marsigli, C., Boccanera, F., Montani, A. and Paccagnella, T., 2005. The COSMO-LEPS
494 mesoscale ensemble system: Validation of the methodology and verification, *Nonlinear Proc.*
495 *Geoph.*, 12, 527–536.
- 496 Miller, M., Buizza, R., Haseler, J., Hortal, M., Janssen, P. and Untch, A., 2010. Increased
497 resolution in the ECMWF deterministic and ensemble prediction systems, *ECMWF*
498 *Newsletter*, 124, 10–16.
- 499 Nash, J. E. and Sutcliffe, J. V., 1970. River flow forecasting through conceptual models part
500 I—A discussion of principles, *J. Hydrol.*, 10, 282–290.
- 501 Ntegeka, V., Salamon, P., Gomes, G., Sint, H., Lorini, V. and Thielen, J., 2013. A high-
502 resolution European dataset for hydrologic modeling, in *EGU General Assembly Conference*
503 *Abstracts*, 15, 7460.
- 504 Pagano, T. C., 2013. Evaluation of Mekong River Commission operational flood forecasts,
505 2000–2012, *Hydrol. Earth Syst. Sci. Discuss.*, 10, 14433–14461, doi:10.5194/hessd-10-
506 14433-2013.

- 507 Pappenberger, F., Ramos, M. H., Cloke, H. L., Wetterhall, F., Alfieri, L., Bogner, K.,
508 Mueller, A., and Salamon, P., submitted. How do I know if my forecasts are better? Using
509 benchmarks in Hydrological Ensemble Predictions, *J. Hydrol.*
- 510 Pappenberger, F., Thielen, J. and Del Medico, M., 2010. The impact of weather forecast
511 improvements on large scale hydrology: analysing a decade of forecasts of the European
512 Flood Alert System, *Hydrol. Process.*, 25, 1091–1113, doi:10.1002/hyp.7772.
- 513 Pappenberger, F., Wetterhall, F., Albergel, C., Alfieri, L., Balsamo, G., Bogner, K., Haiden,
514 T., Hewson, T., Magnusson, L., de Rosnay, P., Muñoz Sabater, J. and Tsonevsky, I., 2013.
515 Floods in Central Europe in June 2013, *ECMWF Newsletter*, 136, 9–11.
- 516 Plate, E. J. and Lindenmaier, F., 2008. Quality assessment of forecasts, in Mekong River
517 Commission: Sixth Annual Flood Forum, Phnom Penh, May, 10 pp.
- 518 Randrianasolo, A., Ramos, M. H., Thirel, G., Andreassian, V. and Martin, E., 2010.
519 Comparing the scores of hydrological ensemble forecasts issued by two different hydrological
520 models, *Atmos. Sci. Lett.*, 11, 100–107, doi:10.1002/asl.259.
- 521 Reed, S., Schaake, J. and Zhang, Z., 2007. A distributed hydrologic model and threshold
522 frequency-based method for flash flood forecasting at ungauged locations, *J. Hydrol.*, 337,
523 402–420.
- 524 Renner, M., Werner, M. G. F., Rademacher, S. and Sprokkereef, E., 2009. Verification of
525 ensemble flow forecasts for the River Rhine, *J. Hydrol.*, 376, 463–475.
- 526 Steppeler, J., Doms, G., Schättler, U., Bitzer, H. W., Gassmann, A., Damrath, U. and
527 Gregoric, G., 2003. Meso-gamma scale forecasts using the nonhydrostatic model LM,
528 *Meteorol. Atmos. Phys.*, 82, 75–96.

- 529 Thielen, J., Bartholmes, J., Ramos, M.-H. and De Roo, A., 2009. The European flood alert
530 system - part 1: Concept and development, *Hydrol. Earth Syst. Sc.*, 13, 125–140.
- 531 Thirel, G., Rousset-Regimbeau, F., Martin, E. and Habets, F., 2008. On the impact of short-
532 range meteorological forecasts for ensemble streamflow predictions, *J. Hydrometeorol.*, 9,
533 1301–1317.
- 534 Trinh, B. N., Thielen-del Pozo, J. and Thirel, G., 2013. The reduction continuous rank
535 probability score for evaluating discharge forecasts from hydrological ensemble prediction
536 systems, *Atmos. Sci. Lett.*, 14, 61–65, doi:10.1002/asl2.417.
- 537 Verkade, J. S., Brown, J. D., Reggiani, P. and Weerts, A. H., 2013. Post-processing ECMWF
538 precipitation and temperature ensemble reforecasts for operational hydrologic forecasting at
539 various spatial scales, *J. Hydrol.*, 501, 73–91, doi:10.1016/j.jhydrol.2013.07.039.
- 540 Wetterhall, F., Pappenberger, F., Alfieri, L., Cloke, H. L., Thielen-del Pozo, J., Balabanova,
541 S., Daňhelka, J., Vogelbacher, A., Salamon, P., Carrasco, I., Cabrera-Tordera, A. J., Corzo-
542 Toscano, M., Garcia-Padilla, M., Garcia-Sanchez, R. J., Ardilouze, C., Jurela, S., Terek, B.,
543 Csik, A., Casey, J., Stankūnavičius, G., Ceres, V., Sprokkereef, E., Stam, J., Anghel, E.,
544 Vladikovic, D., Alionte Eklund, C., Hjerdt, N., Djerv, H., Holmberg, F., Nilsson, J., Nyström,
545 K., Sušnik, M., Hazlinger, M. and Holubecka, M., 2013. HESS Opinions “Forecaster
546 priorities for improving probabilistic flood forecasts,” *Hydrol. Earth Syst. Sci.*, 17, 4389–
547 4399, doi:10.5194/hess-17-4389-2013.
- 548 Wilks, D. S., 2006. *Statistical Methods in the Atmospheric Sciences: An Introduction*,
549 electronic version, Elsevier, San Diego, CA.
- 550 Wittmann, C., Haiden, T. and Kann, A., 2010. Evaluating multi-scale precipitation forecasts
551 using high resolution analysis, *Adv. Sci. Res.*, 4, 89–98.

552 Wood, A. W., Kumar, A. and Lettenmaier, D. P., 2005. A retrospective assessment of
553 National Centers for Environmental Prediction climate model-based ensemble hydrologic
554 forecasting in the western United States, J. Geophys. Res-Atmos., 110,
555 doi:10.1029/2004JD004508.

556

557

ACCEPTED MANUSCRIPT

558 **Tables**

559

560 Table 1: Summary of performance scores and their information content.

Score	Short name	Use
Nash-Sutcliffe efficiency	NS	Normalized measure of the mean squared error of the ensemble mean in comparison to a constant climatological mean
Percent bias	Pbias	Dimensionless measure of the forecast bias
Coefficient of variation of the Root Mean Squared Error	CV	Dimensionless measure of the Root Mean Squared Error of the ensemble mean
Continuous Ranked Probability Skill Score (average discharge as reference)	CRPSS _{ad}	Skill score to compare the distribution of ensemble forecasts around observations, as opposed to using the climatological average discharge
Continuous Ranked Probability Skill Score (persistence forecast as reference)	CRPSS _{pf}	Skill score to compare the distribution of ensemble forecasts around observations, as opposed to using the persistence of the initial discharge

561 **Figure captions**

562

563 Figure 1: Schematic view of the EFAS hydro-meteorological forecasting system.
564

565 Figure 2: stations reporting observed precipitation (left) and average temperature (right) on
566 the 1st October 2013.

567

568 Figure 3: CRPSS_{pf}, CV, NS and Pbias over Europe for 1 year of daily forecasts ending on the
569 1st October 2013 (5-day lead time).

570

571 Figure 4: CRPSS, CV, NS and Pbias of ESP versus the forecast lead time.

572

573 Figure 5: CRPSS_{pf}, CV, NS and Pbias of ESP versus the upstream area of each river grid
574 point.

575

576 Figure 6: Trend of 12-month average CRPSS, CV, NS and Pbias of ESP from 2009 onwards.

577

Figure 1

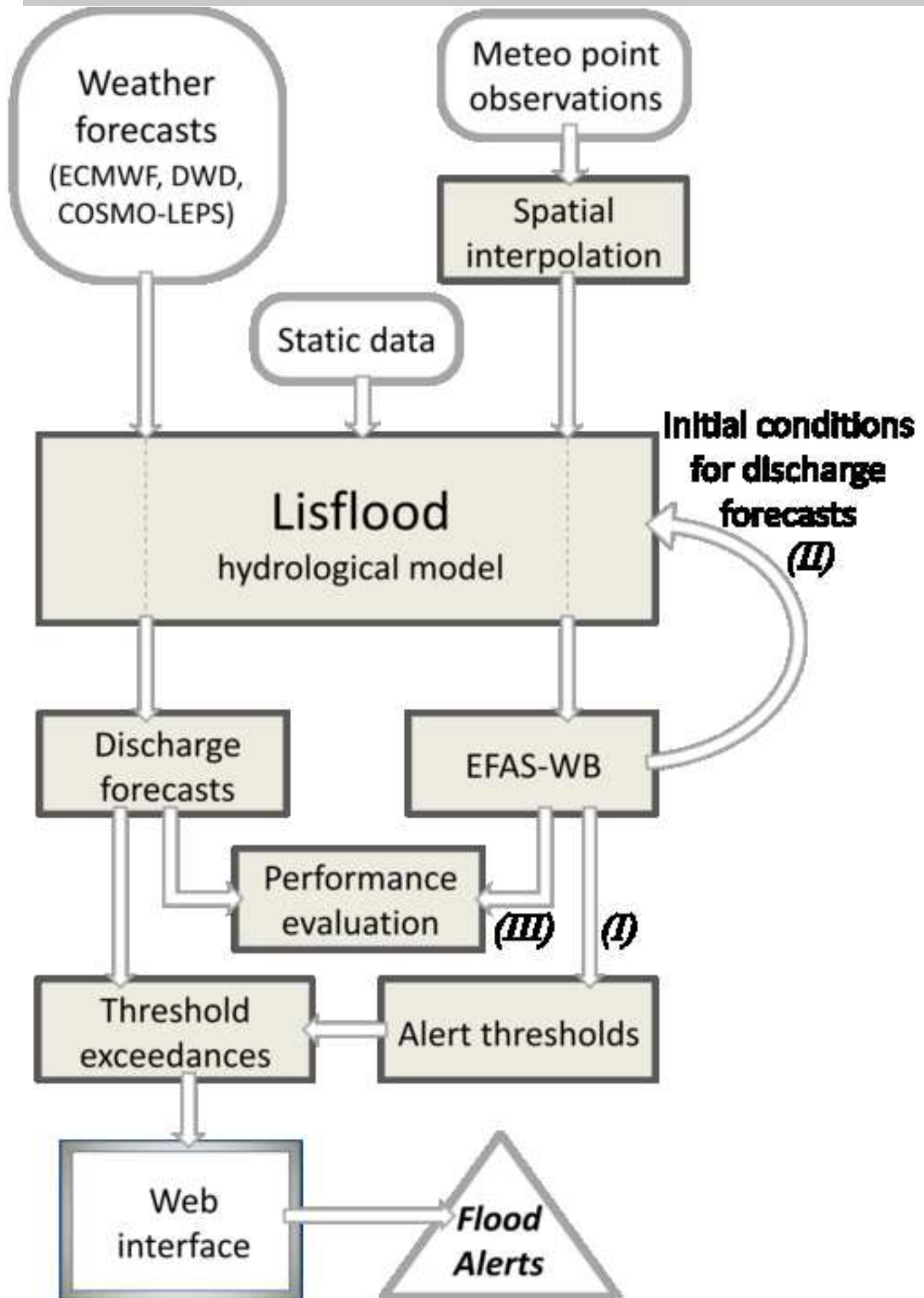
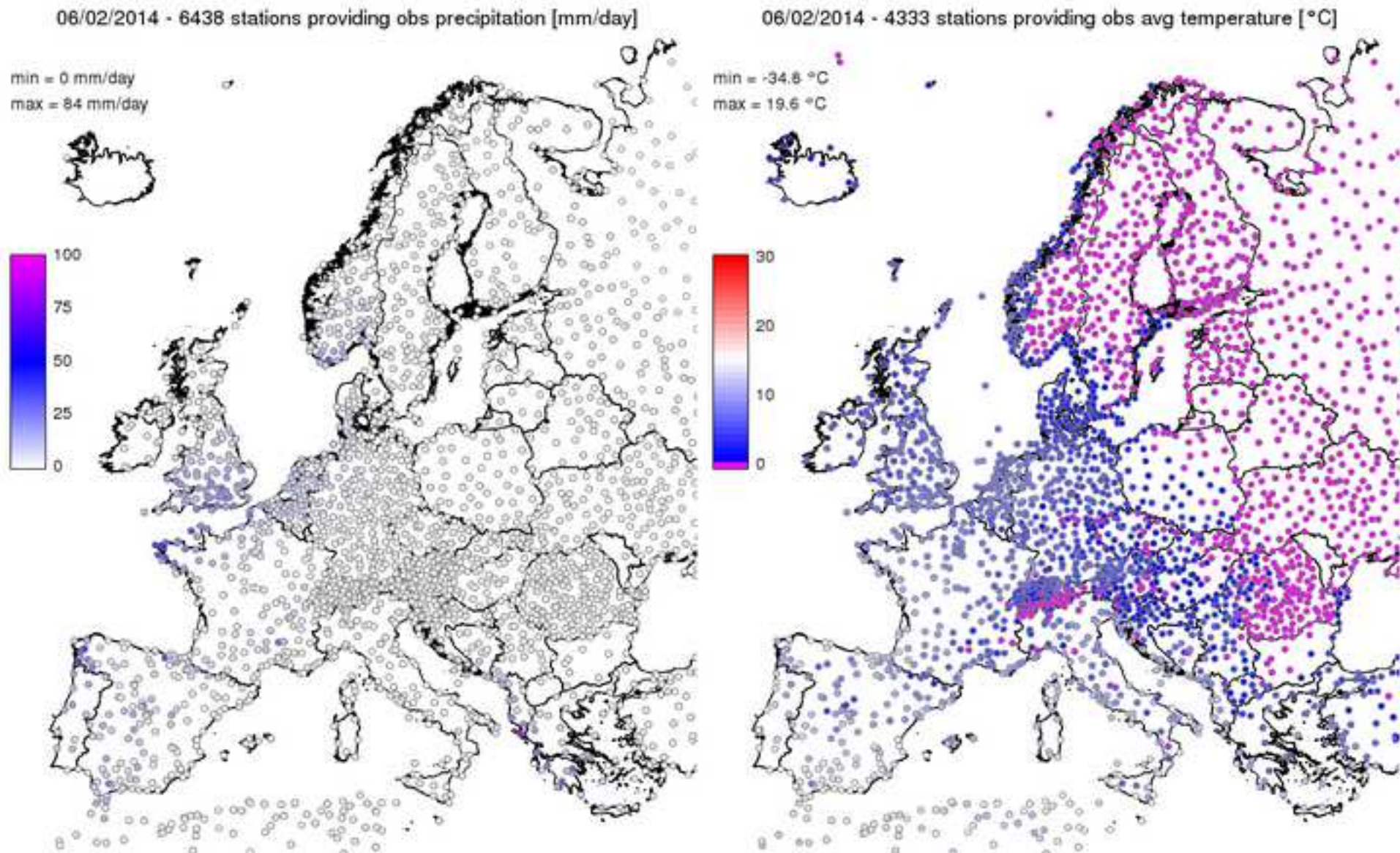
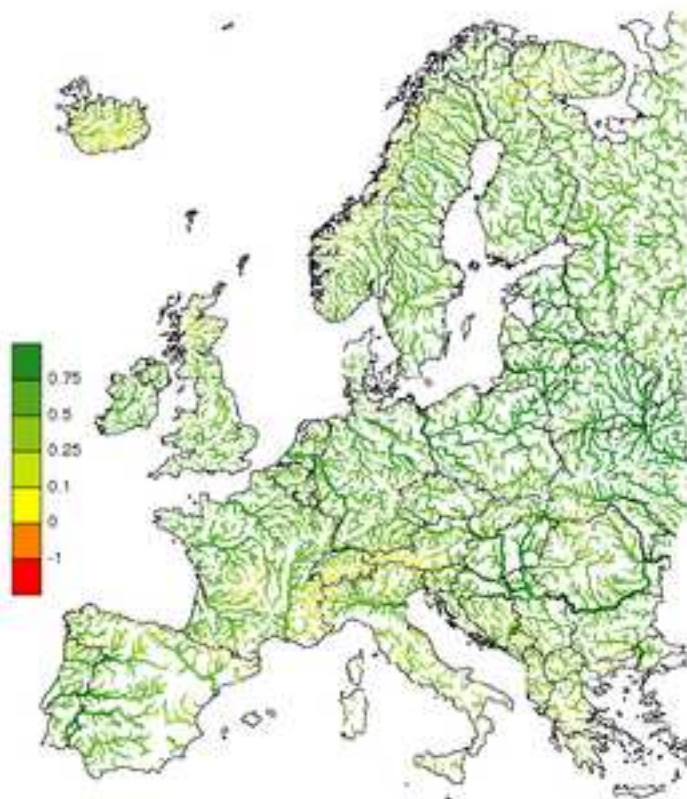


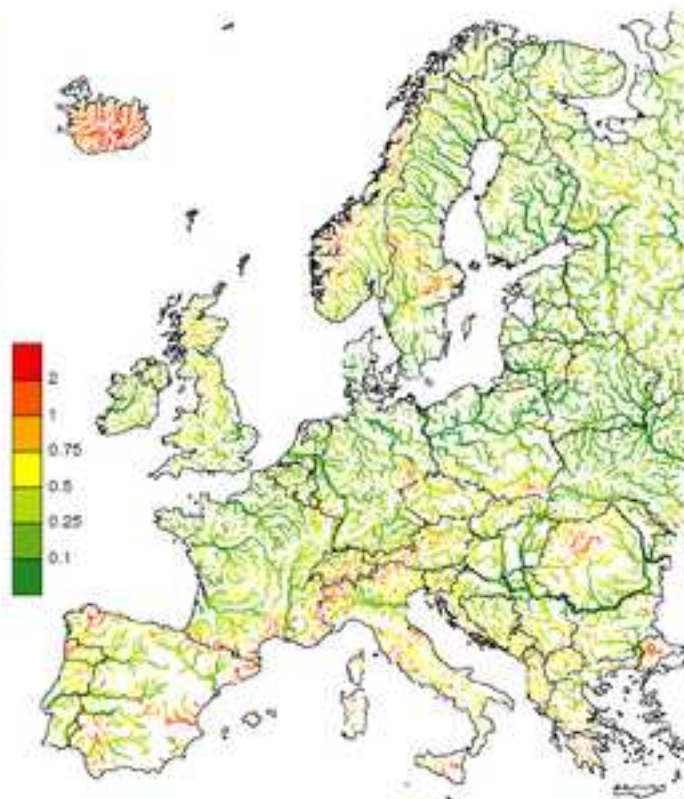
Figure 2



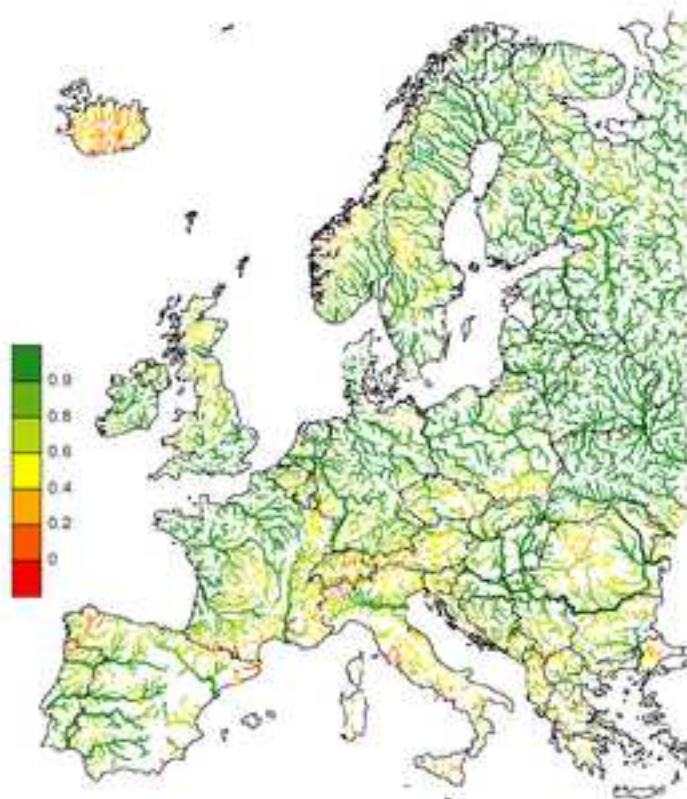
CRPSS - 01/02/2013 to 01/02/2014 - LT = 5 days



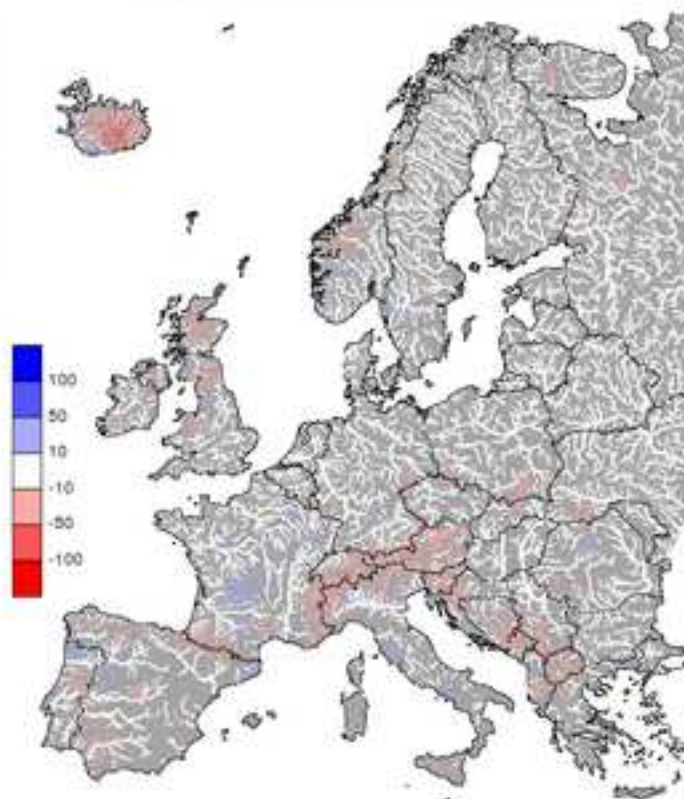
CV of RMSE - 01/02/2013 to 01/02/2014 - LT = 5 days

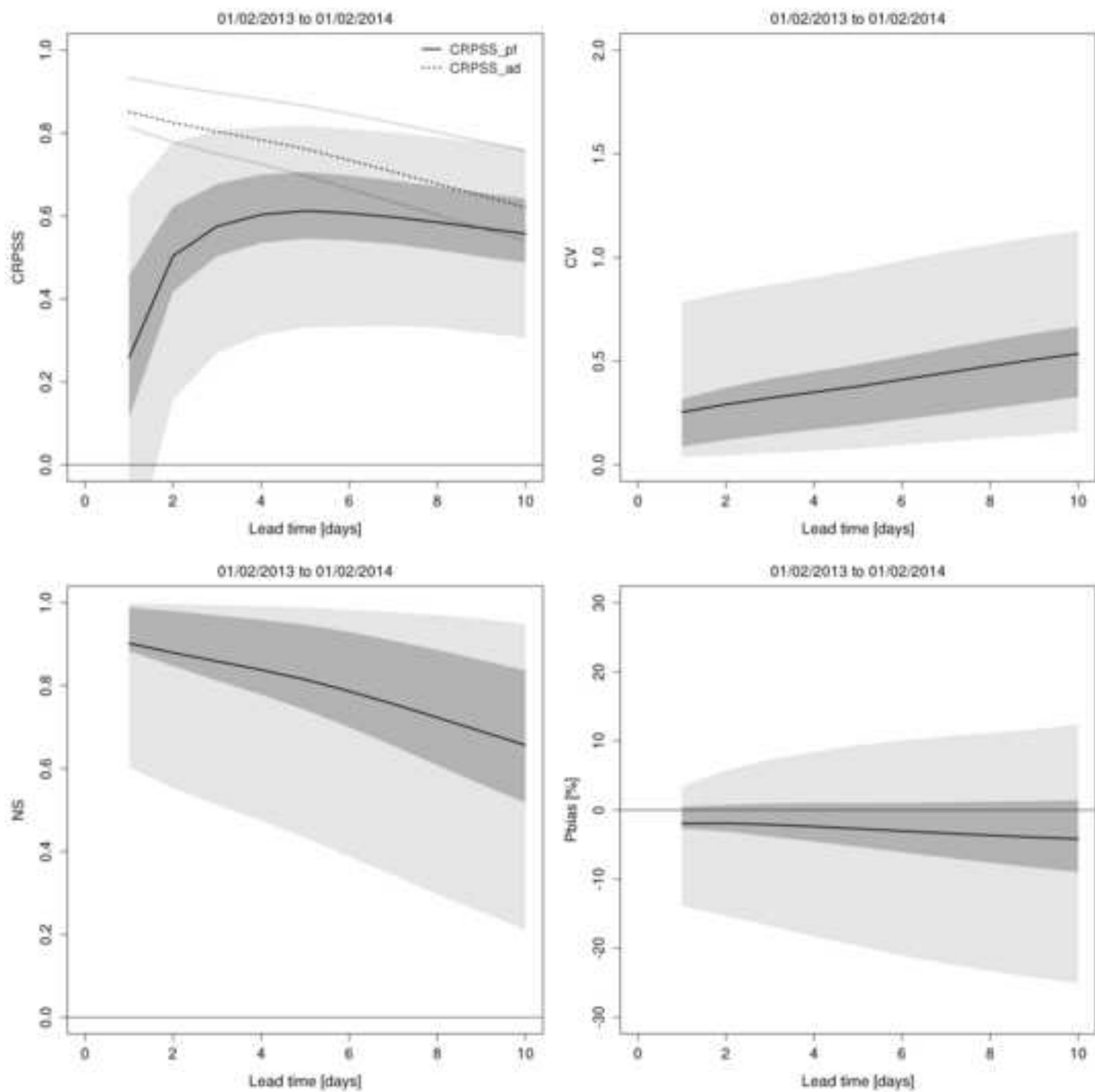


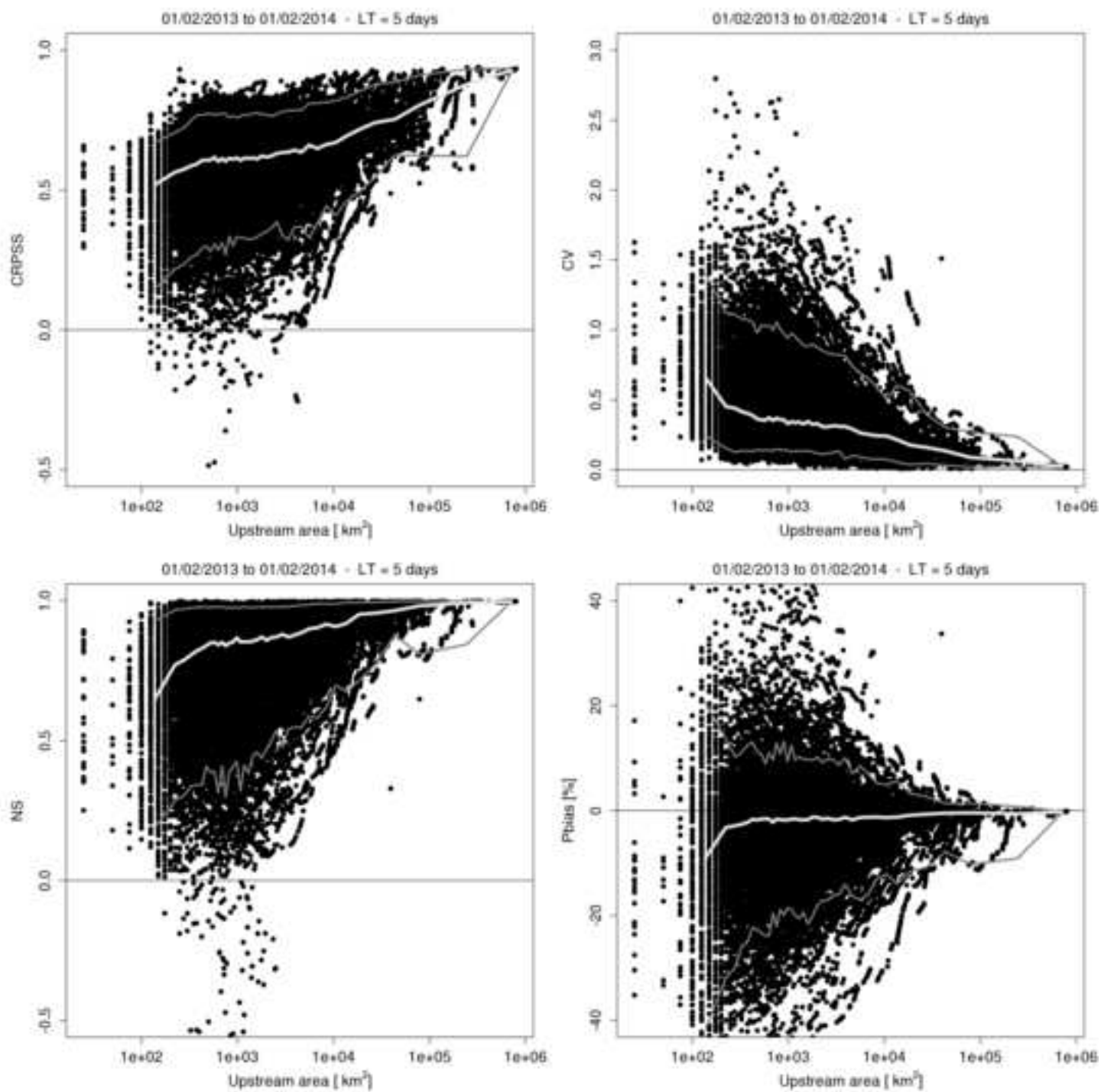
Nash-Sutcliffe - 01/02/2013 to 01/02/2014 - LT = 5 days

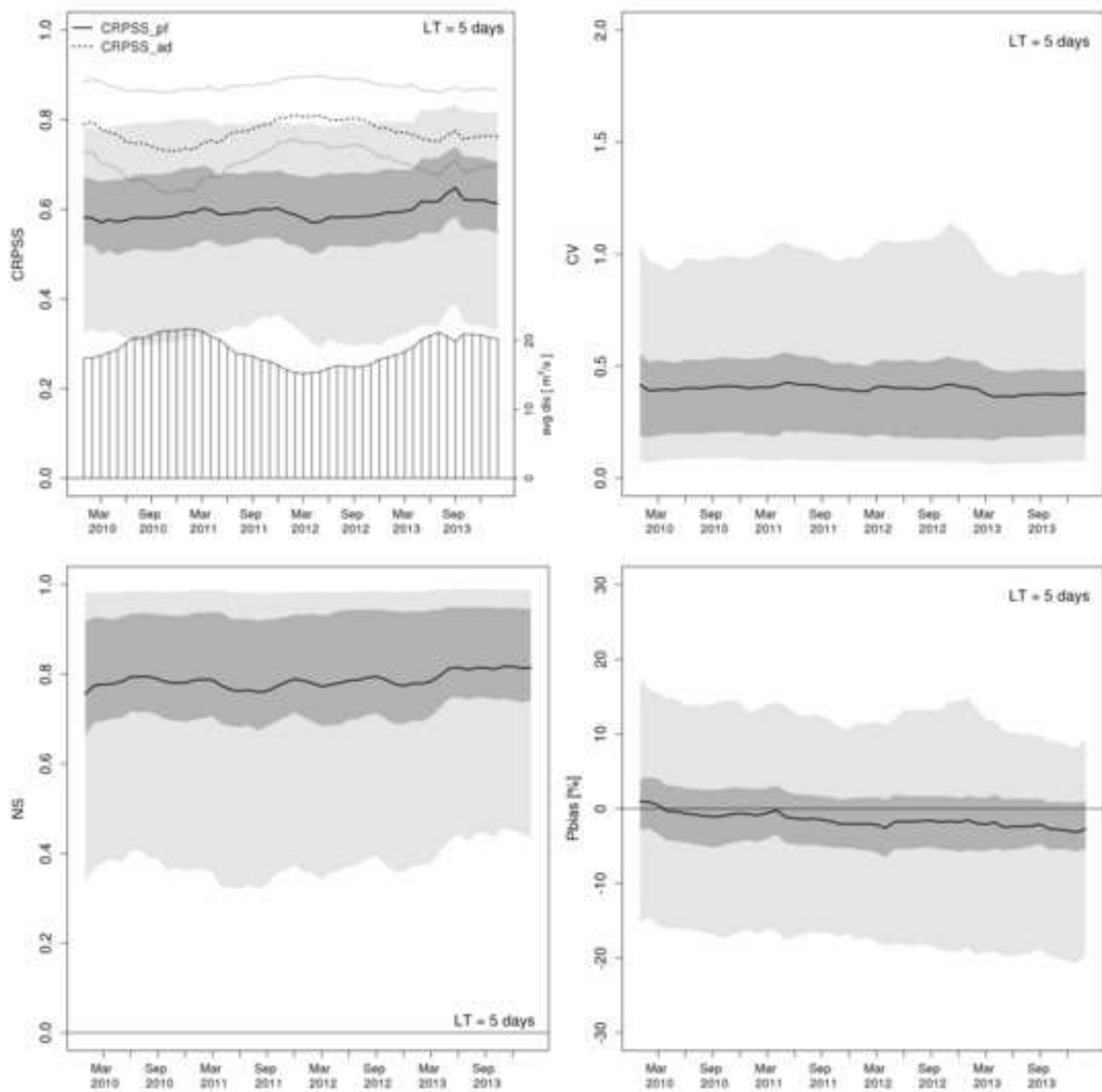


Pbias [%] - 01/02/2013 to 01/02/2014 - LT = 5 days









578

579

Research Highlights

580

581 – The evaluation framework of the European Flood Awareness
582 System is presented

583

584 – Skill scores of ensemble streamflow predictions over Europe are
585 updated regularly

586

587 – Predictions are skillful in river basins larger than 300 km^2 over
588 the 10-day range

589

590 – The use of the CRPSS based on two different references is
591 discussed

592

ACCEPTED MANUSCRIPT